Sliding Mode Control of A Benchmark Cable-Stayed Bridge

Seok J. Moon[1], Lawrence A. Bergman[2] and Petros G. Voulgaris[3]

1. Introduction

The working group on bridge control within the ASCE Committee on Structural Control recently posed a first generation benchmark structural control problem for cable-stayed bridges (Dyke *et al.* 2000), to which this paper responds. Turan (2001) designed three controllers for the benchmark bridge, based on LQG/H2 and μ-synthesis methods. His research showed that the resulting evaluation criteria of the μ-synthesis design were better than those of LQG/H2 designs. While the LQG/H2-based controllers were not robust in performance, the controller designed with μ-tools was robust. The time and frequency responses showed no signs of instability for perturbations of 7%.

In previous research (Moon *et al.* 2001), the authors studied a semi-active system employing MR dampers in conjunction with an LQG/clipped optimal control (LQG/MR) to reduce the structural responses of the benchmark bridge. In this paper, in an effort to improve robustness and performance, sliding mode control (SMC) is applied to the problem, again employing a clipped optimal strategy. The performance and robustness of an SMC-based semi-active control system using MR dampers (SMC/MR) are investigated through a series of numerical simulations and the results were compared with those of LQG/MR and fully active designs.

2. Problem Formulation

2.1 Structural System

The cable-stayed bridge considered for the benchmark study is the Missouri 75-Illinois 146 bridge spanning the Mississippi River near Cape Girardeau, Missouri, designed by the HNTB Corporation. Figure 1 shows the 3-D view of the Cape Girardeau Bridge. A three-dimensional finite element model of the bridge was developed and, from it, an evaluation model of the bridge having 419 DOF was provided by the benchmark problem moderators (Dyke *et al.* 2000). The system matrices obtained through static condensation of the full-order model are given at the

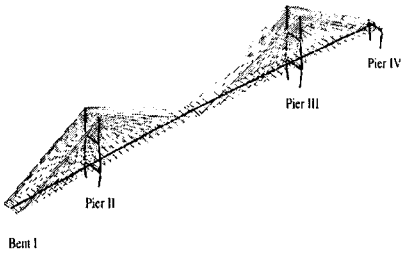

FIGURE 1. 3-D View of the Benchmark Bridge (Turan 2001)

1) Member · Korea Institute of Machinery and Materials, Senior Researcher
2) University of Illinois at Urbana-Champaign, Professor
3) University of Illinois at Urbana-Champaign, Professor

benchmark web site: http://wusceel.cive.wustl.edu/quake.

The equation of motion for the evaluation model can be expressed as

$$M\ddot{U}+C\dot{U}+KU=-M\Gamma\ddot{x}_g+Hf \tag{1}$$

where U is the vector of active DOF, M, C and K are the mass, damping and stiffness matrices of the structural system, respectively, f is the vector of control force inputs, $\ddot{x}_g$ is the longitudinal ground acceleration, Γ is a vector defining the distribution of the ground acceleration to the structural system, and H is a matrix defining how the force(s) produced by the control device(s) enter the structural system. Dissipation in the structural system is defined based on the assumption of modal damping. The damping matrix is developed by assigning 3% of critical damping to each mode.

For computational efficiency, a reduced order model, obtained from the evaluation model, was developed for control design. The reduced order model was formed through balanced realization of the system and condensation of the states with relatively small controllability and observability grammians using the 'balreal' and 'modred' functions in MATLAB . While this resulting model has 30 states, it has the same outputs as the evaluation model. The resulting state equation of the balanced system can be represented as

$$\dot{x}=Ax+B\ddot{x}_g+Ef \tag{2}$$

and the measurement equation and regulated output equation may be obtained as

$$y=C^y x+D^y\ddot{x}_g+F^y f, \quad z=C^z x+D^z\ddot{x}_g+F^z f \tag{3,4}$$

where x, y and z are the state vector, the vector of measured responses and the regulated output vector, respectively.

2.2 MR Damper Modeling

Adequate modeling of the control devices is essential for the accurate prediction of the behavior of the controlled system. A simple phenomenological model for the MR damper is adopted based on the Bouc-Wen model, which is shown to accurately predict the behavior of a shear-mode MR damper over a wide range of inputs (Spencer *et al.* 1997). The equation governing the force predicted by this model is

$$f=c_0\dot{x}_d+\alpha z \tag{5}$$

where x_d is the displacement of the damper, and the evolutionary variable z is governed by

$$\dot{z}=-\gamma|\dot{x}_d|z|z|^{n-1}-\beta\dot{x}_d|z|^n+A\dot{x}_d \tag{6}$$

By adjusting the parameters of the model (γ, β, n, and A), one can control the degree of linearity in

the unloading and the smoothness of the transition from the pre-yield to the post-yield region.

To use the device for control purposes, a model is required that is capable of predicting the behavior of the MR damper for a time-varying command input. Thus, the functional dependence of the parameters on the command voltage was determined. The relations are proposed by Spencer *et al.* (1997). In addition, the resistance and inductance present in the circuit introduces dynamics into the system. These dynamics are observed as a first order time lag in the response of the device to changes in the command input. These dynamics are accounted for through the first order filter.

2.3 Controller Design

The controller is designed to drive the state trajectory into the sliding surface (Utkin 1992, Yang *et al.* 1998). To achieve this goal, a Lyapunov function V is considered,

$$V=\frac{1}{2}S^TS=\frac{1}{2}x^TP^TPx>0 \tag{7}$$

where P is the direction vector of the sliding surface for the control force, which is determined such that the motion on the sliding surface is stable. The first derivative of V with respect to time t is

$$\dot{V}=S^TS=S^TP(Ax+B\ddot{x}_g+Ef) \tag{8}$$

where $\dot{V}$ has to be negative semi-definite for $t<\infty$. To satisfy the negative definiteness condition of $\dot{V}$, the above equation may be modified to

$$\dot{V}=-S^Tdiag(\delta)S\leq 0 \tag{9}$$

where $\delta>0$ is the coefficient of convergence. From the above condition, the control law can be obtained as

$$f=-(PB)^{-1}P(Ax+B\ddot{x}_g)-(PB)^{-1}diag(\delta)Px \tag{10}$$

It is observed that both feedback and feedforward loops are taken account in the design of the controller.

Consider the ith MR damper used to control the structure. As the response of the MR damper is dependent on the relative structural displacements and velocities at the point of attachment, the force generated by the MR damper cannot be commanded; only the voltage v_i applied to the current driver of the ith MR damper can be directly controlled. To induce the MR damper to generate a force approximating the desired optimal control force f_{ci}, an appropriate command signal v_i must be selected. The algorithm for selecting the command signal for the ith MR damper can be concisely written as

$$v_i=V_{\max}H[(f_{ci}-f_i)f_i] \tag{11}$$

where V_{max} is the voltage to the current driver associated with saturation of the MR effect in the tested

device, and H is the Heaviside step function (Dyke *et al.* 1997).

3. Numerical Simulation

The constraints for device force, stroke and velocity are given by max $| f | \leq$ 1000 kN, max $| x_d | \leq$ 2 m, and max $| \dot{x}_d | \leq$ 1 m/sec, respectively. The digitally implemented controller has a sampling time of T = 0.001 sec, which is set equal to the integration time step of the simulation. Each of the measured responses contains an RMS noise of 0.003 V, which is approximately 0.03% of full span of the A/D converters as specified in the control constraints. The measurement noises are modeled as Gaussian rectangular processes with a pulse width of 0.001 sec. Five accelerometers and four displacement sensors are placed on the bridge and control devices. Four accelerometers are located on top of the tower legs (nodes 240, 248, 353, 361), and one is located on the deck at mid span (node 34). All accelerometers are positioned to measure absolute acceleration. Two displacement sensors are positioned between the deck and pier 2 (node pairs (84, 313), (151, 314)), and two displacement sensors are located between the deck and pier 3 (node pairs (118, 428), (185, 429)). All measurements are obtained in the longitudinal direction of the bridge. Also, several load cells are used to measure the control device forces and the earthquake is measured through an accelerometer for feed-forward compensation of SMC strategy. For the design of the observer, the measurement noise is assumed to be independent, identically distributed Gaussian white noise, and $S_{x_i x_i}/S_{v_i v_i} = 25$.

Each control system studied employs a total of 24 control devices between the deck and abutment and the deck and towers, all oriented to apply forces longitudinally. Eight devices are placed between the deck and bent 1, four between the deck and pier 2, eight between the deck and pier 3, and four between the deck and pier 4. Referring to the finite element model (Dyke *et al.* 2000), four devices are located between each of the following pairs of nodes on bent 1 and pier 3: (68, ground), (135, ground), (118, 428), (185, 429); and two devices are located between each of the following pairs of nodes on piers 2 and 4: (84, 313), (151, 314), (134, 444), (201, 440). It is assumed that the devices have a capacity of 1000 kN. MR damper model parameters are used giving dynamic characteristics similar to those of the actual MR damper obtained from experimental data.

3.1 Control Performance of SMC/MR

As a preliminary study, the effects of the sliding margin on the time responses are investigated. The simulation is done by varying the sliding margin over the range {0.1, 1, 5, 15, 25, 35} for the fully active control system: SMC with hydraulic actuator (SMC/HA). Unlike MR dampers, all hydraulic actuators mentioned in this paper are considered to be ideal, and their dynamics are neglected. The values of the evaluation criteria are investigated about base shear, shear at deck level, overturning moment, moment at deck level and cable tension. While the evaluation criteria are generally decreased for increasing sliding margin, some constraints are not satisfied when sliding margin exceeds 35. It is confirmed that control effect is best when the sliding margin is 25. It is thus used as an appropriate value for sliding margin in each succeeding SMC design.

The control performance of SMC/MR for the benchmark problem is demonstrated by numerical simulation with a sampling time of 0.001 sec using a MATLAB/SIMULINK program for the evaluation model. Evaluation of the control performance is carried out using the 18 evaluation criteria

(J_1 ~ J_{18}) provided in the benchmark problem statement for the three different earthquake excitations provided. However, two criteria, J_{14} and J_{15}, are meaningless for semi-active systems.

Table 1 shows the values of the evaluation criteria provided in the benchmark statement. For comparison, another semi-active system and two fully active systems are also considered: LQG-based semi-active system using MR dampers (LQG/MR, Moon *et al.* 2001), LQG system with hydraulic actuators (LQG/HA) provided by the benchmark moderators as a sample control design, and SMC/HA. In each case, tension in the stay cables remained within the recommended region of allowable values. The tension in the *i*th cable may not exceed 0.7 T_{fi} or fall below 0.2 T_{fi}, where T_{fi} is the tension that would cause failure of the *i*th cable. The base force responses of the controlled bridge are compared to those of the uncontrolled bridge for the El Centro, Mexico City, and Gebze earthquakes in Figure 2. Note that each controller is able to achieve a significant reduction in the base shear force when compared with the uncontrolled system. Compared with the uncontrolled responses, the base shears in SMC/MR are reduced to 39~45 % levels in the peak values (J_1) and to 22~37 % levels in the normed values (J_7) for the three earthquake excitations. Overturning moments are reduced to 30~49 % levels in the peak values (J_3) and to 19~38 % level in the normed values (J_9). It is clear that most of the structural responses generated by the El Centro earthquake are controlled well. Further, the numerical results show that the SMC/MR system performs slightly better than the two active systems, SMC/HA and LQG/HA. All of the evaluation criteria representing the structural responses due to the Mexico City earthquake are found to be in the range of 64.3~94.9 % of results from LQG /HA. Device stroke (J_{13}) is approximately 64.5~92.5 % of that of two active systems. On the other hand, while the SMC gives better performance than the LQG control on the benchmark bridge problem in comparison with the two active systems, both of the semi-active systems, SMC/MR and LQG/MR, give nearly equal performance.

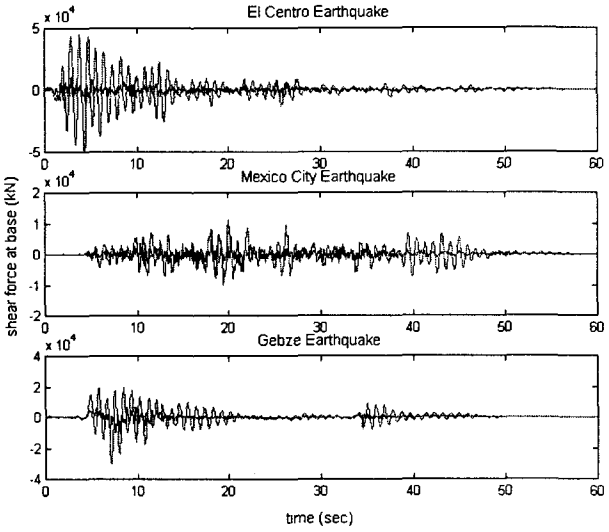

FIGURE 2. Controlled Shear Forces at Base Level against Three Different Earthquakes

To demonstrate the feasibility of each controller, peak values of the force, stroke, and velocity are provided for each earthquake in Table 2. Here, it is confirmed that the results satisfy all of the required constraints for the control devices.

3.2 Controller Robustness to Stiffness Uncertainty

The dynamic characteristics of the real bridge might not be expected to be identical to the evaluation model provided by the benchmark moderators. Even if the designed controller was confirmed to have

good performance in the evaluation model, it would not necessarily mean that it would yield good performance in the actual system. Furthermore, the controller was designed as a linear one about the linearized deformed state of the bridge under its own weight. The highly non-linear behavior of cable-stayed bridges could cause the structural stiffness and the damping matrices to change during large deformations of the bridge. These non-linear aspects were not taken into account during the design process of the controller.

Therefore, the robustness of SMC/MR is investigated with respect to the uncertainties of stiffness parameter. The stiffness matrix is perturbed by some amount, and the resulting bridge model is simulated with the controller designed for the nominal system. The resulting perturbed stiffness is calculated as

$$K_{pert} = K(1+\varepsilon) \tag{12}$$

where K is the nominal stiffness of the bridge, which was used in the formulation of the evaluation model and for which the controller is designed, ε is the perturbation amount, and K_{pert} is the perturbed stiffness matrix. Perturbations of 7 % and 30 % are considered. The evaluation criteria results for the unperturbed and the 7 % stiffness perturbed systems under El Centro earthquake are summarized in Table 3. It also includes the results of the μ-synthesis controller (Turan 2001) and maximum variation on each criterion. These values make it clear that SMC/MR controller works well and is more robust for stiffness matrix perturbations than μ-synthesis. Table 4 shows the values of evaluation criteria for 30 % perturbed systems under three earthquake excitations. It is confirmed that SMC/MR is robust for uncertainties of stiffness parameter of the bridge under various earthquake loading.

4. Conclusions

The sliding mode control is adopted to improve control effect and to enhance robustness. The effectiveness of the SMC-based semi-active control system using MR damper (SMC/MR) in reducing structural responses for a wide range of seismic loading conditions has been demonstrated through a series of numerical studies of the benchmark cable-stayed bridge problem. The numerical results show that SMC/MR can suppress the vibration of the seismically excited cable-stayed bridge structure effectively. A comparison of results with two fully active systems using hydraulic actuators indicates SMC/MR to be more effective than the active control systems. Robustness of SMC/MR is investigated with respect to uncertainties in stiffness. For 7% perturbed systems, and even for 30% perturbed systems, SMC/MR is stable and performs well.

With this study, we confirm the capability and robustness of the MR damper-based system, semi-active MR damper system using sliding mode control, for seismic response reduction in cable-stayed bridge structures.

Acknowledgments

This research is supported in part by Korea Ministry of Science & Technology as a National Research Laboratory project.

References

1. Dyke, S.J., Spencer, B.F., Sain, M.K. and Carlson J.D. (1997) An Experimental Study of MR Dampers for Seismic Protection. *Smart Materials and Structures: Special Issue on Large Civil Structures.*
2. Dyke, S.J., Turan, G., Caicedo, J.M., Bergman, L.A. and Hague S. (2000) Benchmark Control Problem for Seismic Response of Cable-Stayed Bridges. .
3. Moon, S.J., Bergman, L.A. and Voulgaris P.G. (2001) Application of Megnetorheological Dampers to Control of a Cable-Stayed Bridge Subjected to Seismic Excitation. Technical Report, University of Illinois, Urbana, IL.
4. Spencer, B.F., Dyke, S.J., Sain, M.K. and Carlson, J.D. (1997) Phenomenological Model of a Magnetorheological Damper. *Journal of Engineering Mechanics ASCE* 123 (3), 230-238.
5. Turan, G. (2001) Active Control of a Cable-Stayed Bridge Against Earthquake Excitations. *Ph.D. Thesis*. University of Illinois at Urbana-Champaign, IL.
6. Utkin, V.I. (1992) *Sliding Modes in Control Optimization,* Springer, New York, NY.
7. Yang, J.N., Samali, B., and Agrawal, A.K. (1998) Sliding Mode Control with Compensator for Wind and Seismic Response Control. *Earthquake Engineering and Structural Dynamics* 27 (11), 1141-1147

Table 1. Comparisons of Evaluation Criteria

Type	Controller	J_1			J_2			J_3		
		El Centro	Mexcio	Gebze	El Centro	Mexcio	Gebze	El Centro	Mexcio	Gebze
Smi-Active	SMC/MR	0.397	0.453	0.392	1.090	1.068	1.146	0.300	0.488	0.382
	LQG/MR	0.391	0.469	0.415	1.084	1.179	1.376	0.267	0.466	0.395
Active	SMC/HA	0.411	0.401	0.398	1.087	0.956	1.182	0.306	0.490	0.364
	LQG/HA	0.401	0.477	0.450	1.093	1.258	1.379	0.301	0.564	0.434
Type	Controller	J_4			J_5			J_6		
		El Centro	Mexcio	Gebze	El Centro	Mexcio	Gebze	El Centro	Mexcio	Gebze
Smi-Active	SMC/MR	0.557	0.408	1.053	0.205	0.056	0.159	0.880	1.578	2.941
	LQG/MR	0.485	0.398	0.940	0.194	0.062	0.142	0.852	1.373	2.521
Active	SMC/HA	0.688	0.578	1.071	0.193	0.052	0.139	1.327	2.418	3.176
	LQG/HA	0.602	0.635	1.385	0.189	0.073	0.161	1.089	2.446	4.067
Type	Controller	J_7			J_8			J_9		
		El Centro	Mexcio	Gebze	El Centro	Mexcio	Gebze	El Centro	Mexcio	Gebze
Smi-Active	SMC/MR	0.217	0.372	0.286	0.903	0.902	1.271	0.193	0.315	0.380
	LQG/MR	0.227	0.443	0.318	0.924	1.131	1.329	0.209	0.383	0.389
Active	SMC/HA	0.224	0.362	0.282	0.896	0.958	1.183	0.193	0.329	0.356
	LQG/HA	0.229	0.439	0.326	1.113	1.209	1.509	0.233	0.417	0.469
Type	Controller	J_{10}			J_{11}			J_{12}		
		El Centro	Mexcio	Gebze	El Centro	Mexcio	Gebze	El Centro	Mexcio	Gebze
Smi-Active	SMC/MR	0.577	0.720	1.487	0.018	0.006	0.012	1.96e-3	1.96e-3	1.96e-3
	LQG/MR	0.556	0.642	1.202	0.019	0.006	0.013	1.96e-3	1.96e-3	1.96e-3
Active	SMC/HA	0.585	0.888	1.256	0.016	0.006	0.011	1.96e-3	1.96e-3	1.96e-3
	LQG/HA	0.732	1.025	1.617	0.024	0.009	0.018	1.96e-3	0.68e-3	1.96e-3
Type	Controller	J_{13}			J_{16}			J_{17} / J_{18}		
		El Centro	Mexcio	Gebze	El Centro	Mexcio	Gebze	El Centro	Mexcio	Gebze
Smi-Active	SMC/MR	0.578	0.795	1.612	24	24	24	17 / 30	17 / 30	17 / 30
	LQG/MR	0.559	0.692	1.382	24	24	24	17 / 30	17 / 30	17 / 30
Active	SMC/HA	0.871	1.218	1.741	24	24	24	9 / 30	9 / 30	9 / 30
	LQG/HA	0.715	1.232	2.230	24	24	24	9 / 30	9 / 30	9 / 30

Table 2. Comparisons of Actuator Requirements

Max. Force (kN) / Max. Stroke (m) / Max. Velocity (m/s)			
Controller	El Centro	Mexico	Gebze
SMC/MR	1000.00 / 0.10 / 0.67	1000.00 / 0.03 / 0.20	1000.00 / 0.25 / 0.60
LQG/MR	1000.00 / 0.09 / 0.54	1000.00 / 0.03 / 0.24	1000.00 / 0.18 / 0.49
SMC/HA	1000.00 / 0.14 / 0.95	607.11 / 0.07 / 0.46	1000.00 / 0.42 / 0.67
LQG/HA	1000.00 / 0.10 / 0.71	318.40 / 0.05 / 0.35	934.00 / 0.26 / 0.58

Table 3. Evaluation Criteria for ±7% stiffness Perturbed Systems under El Centro Earthquake

E.C.	μ-Synthesis (Using 32 Control Devices)				SMC/MR (Using 24 Control Devices)			
	ε = 0.0	ε = +0.07	ε = -0.07	Max. Variation	ε = 0.0	ε = +0.07	ε = -0.07	Max. Variation
J_1	0.360	0.376	0.493	36.9%	0.394	0.353	0.432	10.4%
J_2	0.712	0.909	1.082	52.0%	1.130	1.005	1.323	17.1%
J_3	0.280	0.272	0.343	22.5%	0.296	0.256	0.335	13.5%
J_4	0.503	0.518	0.659	31.0%	0.560	0.527	0.540	5.9%
J_5	0.185	0.184	0.168	9.2%	0.213	0.197	0.224	7.5%
J_6	0.962	0.979	1.145	19.0%	0.870	0.793	0.862	8.9%
J_7	0.424	0.470	0.625	47.4%	0.218	0.207	0.235	7.8%
J_8	1.095	1.482	1.333	35.3%	0.887	0.880	0.901	1.6%
J_9	0.395	0.422	0.509	28.5%	0.189	0.180	0.198	4.8%
J_{10}	0.970	1.221	1.151	18.7%	0.551	0.515	0.556	6.5%
J_{11}	0.032	0.042	0.037	31.3%	0.016	0.016	0.017	6.3%

Table 4. Evaluation Criteria for ±30% Stiffness Perturbed System

	El Centro Earthquake			Mexico City Earthquake			Gebze Earthquake			Max. Variation
ε	0.00	+0.30	-0.30	0.00	+0.30	-0.30	0.00	+0.30	-0.30	
J_1	0.397	0.249	0.424	0.453	0.377	0.558	0.392	0.327	0.473	37.3%
J_2	1.090	0.784	1.632	1.068	0.958	1.474	1.146	0.876	1.712	58.4%
J_3	0.300	0.200	0.339	0.488	0.413	0.587	0.382	0.262	0.498	33.3%
J_4	0.557	0.451	0.686	0.408	0.519	0.457	1.053	1.015	1.380	31.1%
J_5	0.205	0.154	0.236	0.056	0.055	0.060	0.159	0.109	0.196	31.4%
J_6	0.880	0.914	1.045	1.578	1.734	1.641	2.941	2.737	3.309	18.8%
J_7	0.217	0.180	0.312	0.372	0.314	0.495	0.286	0.241	0.402	43.8%
J_8	0.903	0.747	1.054	0.902	0.909	1.195	1.271	1.081	1.856	46.0%
J_9	0.193	0.153	0.246	0.315	0.299	0.410	0.380	0.322	0.527	38.7%
J_{10}	0.577	0.468	0.594	0.720	0.761	0.783	1.487	1.316	1.997	34.3%
J_{11}	0.018	0.015	0.019	0.006	0.007	0.007	0.013	0.009	0.023	76.9%
J_{12}	0.0020	0.0020	0.0020	0.0020	0.0020	0.0020	0.0020	0.0020	0.0020	0.0%
J_{13}	0.578	0.560	0.686	0.795	0.873	0.826	1.612	1.500	1.814	18.7%